Histone modifications affect timing of oligodendrocyte progenitor differentiation in the developing rat brain

Siming Shen, Jiadong Li, and Patrizia Casaccia-Bonnefil

Department of Neuroscience and Cell Biology, R. Wood Johnson Medical School, Piscataway, NJ 08854

Timely differentiation of progenitor cells is critical for development. In this study we asked whether global epigenetic mechanisms regulate timing of progenitor cell differentiation into myelin-forming oligodendrocytes in vivo. Histone deacetylation was essential during a specific temporal window of development and was dependent on the enzymatic activity of histone deacetylases, whose expression was detected in the developing corpus callosum. During the first 10 postnatal days, administration of valproic acid (VPA), the specific inhibitor for histone deacetylase activity, resulted in significant hypomyelination with delayed expression of late differentiation markers and retained expression of progenitor markers. Differentiation resumed in VPA-injected rats if a recovery period was allowed. Administration of VPA after myelination onset had no effect on myelin gene expression and was consistent with changes of nucleosomal histones from reversible deacetylation to more stable methylation and chromatin compaction. Together, these data identify global modifications of nucleosomal histones critical for timing of oligodendrocyte differentiation and myelination in the developing corpus callosum.

Introduction

The identification of mechanisms modulating timing of cellular differentiation is critical for morphogenesis and proper development. In this study we have addressed this issue in the oligodendrocyte (OL) lineage. OLs are the myelin-forming cells of the central nervous system and they derive from progenitor cells generated by multipotent precursors. The concept of timing of OL differentiation was originally proposed based on very elegant studies on cultured progenitors purified from the optic nerve (Temple and Raff, 1986). Since then, other studies have confirmed, refuted, or modified this concept (Barres et al., 1994; Ibarrola et al., 1996) and attempts have been made to identify the molecular "effectors" of the timing mechanism. In studies on progenitors from the developing optic nerve, for instance, it had been proposed that timing of OL differentiation was linked to cell cycle exit and that the cell cycle inhibitor p27Kip1 was a major component of the timing mechanism (Durand et al., 1997, 1998; Durand and Raff, 2000). This hypothesis implied that OL differentiation proceeded by default once the cells exited from the cell cycle. However, overexpression of p27Kip1 in vitro was not sufficient to initiate OL differentiation (Tikoo et al., 1998; Tang et al., 2000), and in vivo phenotypic analysis of the p27Kip1 null mice revealed no delay in timing of myelination (Casaccia-Bonnefil et al., 1997, 1999). Additional studies have suggested the role of transcriptional inhibitors such as the basic helix-loop-helix molecules Id2 (Wang et al., 2001), Id4 (Kondo and Raff, 2000b), and Hes5 (Kondo and Raff, 2000b). However, it is unlikely that any single component could recapitulate the process of timely OL differentiation.

The premise of this study is that the progression along the OL lineage is a complex event characterized by global changes in gene expression, resulting in loss of precursor markers and differentiation inhibitors and acquisition of late differentiation markers, including enzymes for the synthesis of myelin lipids and myelin proteins, such as ceramide-galactosyl-transferase (CGT), myelin basic protein (MBP), and myelin-associated glycoprotein (MAG). We had previously reported that global changes affecting deacetylation of nucleosomal histones were critical for OL differentiation in vitro (Marin-Husstege et al., 2002). Reversible acetylation of selected lysine residues in the conserved tails of nucleosomal core histone proteins represents an efficient way to regulate gene expression (for reviews see Strahl and Allis, 2000; Turner, 2000; Yoshida et al., 2003; Yang, 2004). In general, increased histone acetylation (hyperacetylation) is associated with increased transcriptional activity, whereas decreased acetylation

Correspondence to Patrizia Casaccia-Bonnefil: casaccpa@umdnj.edu

Abbreviations used in this paper: AcH3, acetylated histone H3; AcLys, acetyllysine; CGT, ceramide-galactosyl-transferase; HAT, histone acetyltransferase; HDAC, histone deacetylase; MAG, myelin-associated glycoprotein; MBP, myelin basic protein; MeK9H3, methylated lysine 9 on histone H3; OL, oligodendrocyte; TSA, trichostatin A; VPA, valproic acid.

The Journal of Cell Biology, Vol. 169, No. 4, May 23, 2005 577–589
http://www.jcb.org/cgi/doi/10.1083/jcb.200412101

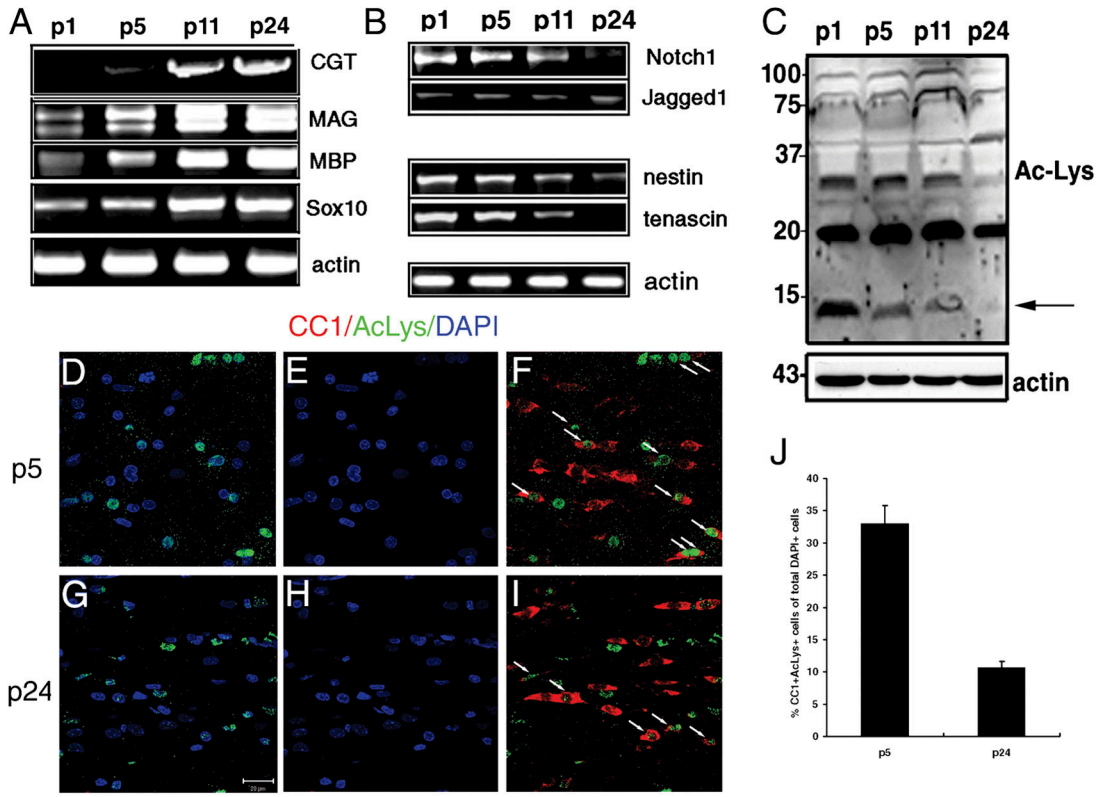

Figure 1. **Global changes of gene expression in the developing corpus callosum correlated with decreased protein acetylation.** (A) RT-PCR of total RNA extracted from the anterior corpus callosum of p1, p5, p11, and p24 rats and amplified with primers for CGT, MAG, MBP, and Sox10 and actin. (B) RT-PCR of total RNA amplified with primers for Notch-1, Jagged-1, nestin, tenascin, and actin. (C) Western blot of protein extracted from the anterior corpus callosum at the indicated time points and probed with anti-acetyl-lysine (AcLys) antibodies. Actin was used as loading control. Note the deacetylation of the14-kD band (arrow) occurring at the onset of myelination. (D–I) Coronal brain sections from p5 (D–F) and p24 (G–I) were stained with AcLys (D, F, G, and I, green), CC1 (F and I, red), and DAPI (blue) as counterstain. Bar, 20 μm. 63× objective, LSM510 microscope (Carl Zeiss MicroImaging, Inc.). Double-labeled CC1+/AcLys+ cells (F and I, white arrows) were counted within the same area of the medial corpus callosum at each time point and referred to the total number of CC1+ cells. The differences between the two time points were statistically different ($P < 0.001$) (J). These data are representative of at least three independent experiments using three individual rat pups for each time point.

(hypoacetylation or deacetylation) is associated with repression of gene expression (Forsberg and Bresnick, 2001; Wade 2001).

The removal of acetyl groups from lysine residues in the histone tails is performed by specific enzymes called histone deacetylases (HDACs) that can be broadly grouped into three major classes. Class I includes HDAC-1, -2, -3, and -8 and is composed of small proteins (377–488 aa), sharing sequence homology to the yeast transcriptional regulator RPD3 (Bjerling et al., 2002), and a broad expression pattern. Class II includes HDAC-4, -5, -6, -7, and -9 and is composed of proteins of larger size (669–1215 aa), sharing sequence homology with the yeast HDA1 (Fischle et al., 2002), and a restricted expression pattern (de Ruijter et al., 2003). Class III HDACs, the Sir2 family proteins, includes molecules that are sensitive to the redox state of the cell and are inhibited by a different category of pharmacological inhibitors (Grozinger et al., 2001) than the other two classes (Phiel et al., 2001; Gottlicher, 2004; Gurvich et al., 2004).

Because the acetylation state of nucleosomal histones modulates chromatin structure and epigenetically regulates gene expression, we hypothesized that this could be the global mechanism responsible for timing of OL progenitor differentiation in vivo. We addressed this question in the developing corpus callosum because timing of myelination of this region has been thoroughly characterized (Bjelke and Seiger, 1989; Hamano et al., 1996, 1998) and because of its functional relevance as the major myelinated fiber tract of the adult brain. The corpus callosum is composed of millions of fibers that need to be properly myelinated to allow communication between the two brain hemispheres. Myelination in this structure follows a precise timing, during the first two postnatal weeks of development (Bjelke and Seiger, 1989; Hamano et al., 1996, 1998), and a precise topology, starting at caudal levels and progressing rostrally (Smith, 1973) and starting laterally and proceeding medially (Smith, 1973).

In this study we asked whether deacetylation occurred in OL progenitors residing in the developing anterior corpus callosum and whether inhibition of this process in vivo would affect timing of myelination.

Results

Global changes in gene expression correlate with progressive histone deacetylation in the developing corpus callosum

OL differentiation in the rostral corpus callosum was characterized by the synthesis of late differentiation markers including

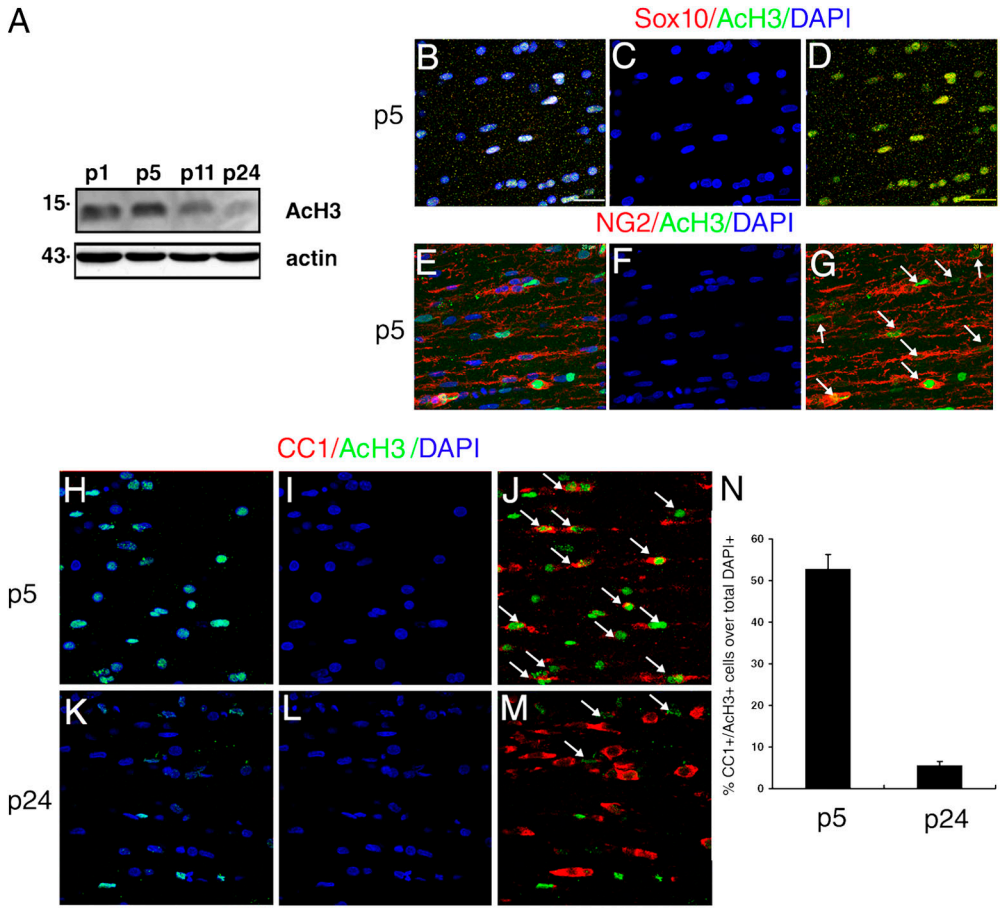

Figure 2. **Histone H3 acetylation in OL progenitors of the medial corpus callosum progressively decreased during postnatal development.** The 14-kD protein undergoing deacetylation during the first two postnatal days was identified by Western blot analysis using antibodies recognizing acetylated histone H3 (AcH3) and actin as loading control (A). To confirm that AcH3 was present in the nuclei of cells of the OL lineage, brain sections were labeled with antibodies against AcH3 (B, D, E, and G, green), Sox10 (B and D, red), NG2 (E and G, red), and DAPI (blue) as nuclear counterstain. Bar, 20 μm. 63× objective, LSM510 microscope (Carl Zeiss MicroImaging, Inc.). Double-positive cells are indicated by white arrows. (H–M) Confocal images of the medial corpus callosum at p5 and p24 stained for AcH3 (H, J, K, and M, green), CC1 (J and M, red), and DAPI (blue). Compare the similar density of DAPI+ nuclei with the decrease of CC1+/AcH3+ cells (J and M, white arrows). The CC1+/AcH3+ cells were counted and referred to the total number of CC1+ cells (N). The bar graph shows the statistically significant ($P < 0.001$) decrease of AcH3+/CC1+ cells from p5 to p24.

MBP, MAG, and CGT, the progressive increase of the transcription factor Sox10 (Fig. 1 A), and the loss of precursor markers including tenascin, nestin, and Notch1 (Fig. 1 B). Because OL differentiation was associated with such generalized changes in progenitors, we hypothesized that global changes affecting chromatin components could modulate timing of myelination in the corpus callosum by modulating gene expression. Histone acetylation is one of the best-characterized mechanisms of regulating gene expression, and we therefore investigated whether it occurred in the developing corpus callosum. Several acetylated proteins ranging between 10 and 100 kD were detected in Western blot analysis of protein extracts from the rostral corpus callosum at postnatal day 1 (p1), p5, p11, and p24 (Fig. 1 C). Of these bands, only the 14- and the 30-kD protein displayed a distinctive temporal pattern of deacetylation. The 30-kD band lost its acetyl groups only during the third postnatal week (Fig. 1 C). Deacetylation of the 14-kD band, in contrast, started at p5 and continued throughout the period coincident with the onset of myelination. The acetylation level of this protein, therefore, correlated with high expression of progenitor markers and progressively decreased during OL differentiation. The occurrence of protein acetylation in OL lineage cells in the medial region of the body of the corpus callosum was confirmed by immunohistochemistry using the antibody recognizing the OL differentiation marker CC1 (Fig. 1, D–I). At p5, the number of double-positive CC1+/AcLys+ cells was 917 ± 29 per mm^2 ($n = 3$), corresponding to 68.7% of the total number of CC1+ cells per mm^2 (x = 1334 ± 57; $n = 3$). At p24, in contrast, the number of CC1+/AcLys+ double-positive cells was 384 ± 29, corresponding to 27% of the total number of CC1+ cells per mm^2 (x = 1384 ± 29; $n = 3$) (Fig. 1 J). The 14-kD band corresponded to acetylated histone H3 (AcH3), as determined by Western blot analysis (Fig. 2 A), and the presence of AcH3 in the nuclei of OL progenitors in the developing corpus callosum was further characterized by immunofluorescence for the marker Sox10 (Fig. 2, B–D) and NG2 (Fig. 2, E–G). Remarkably, in the medial region of the body of the corpus callosum at rostral levels, the majority of the Sox10+ cells (Fig. 2 D) and of the NG2+ cells (Fig. 2 G) were also AcH3. To confirm the progressive decrease in AcH3 during OL development, we also processed p5 and p24 brain sections for

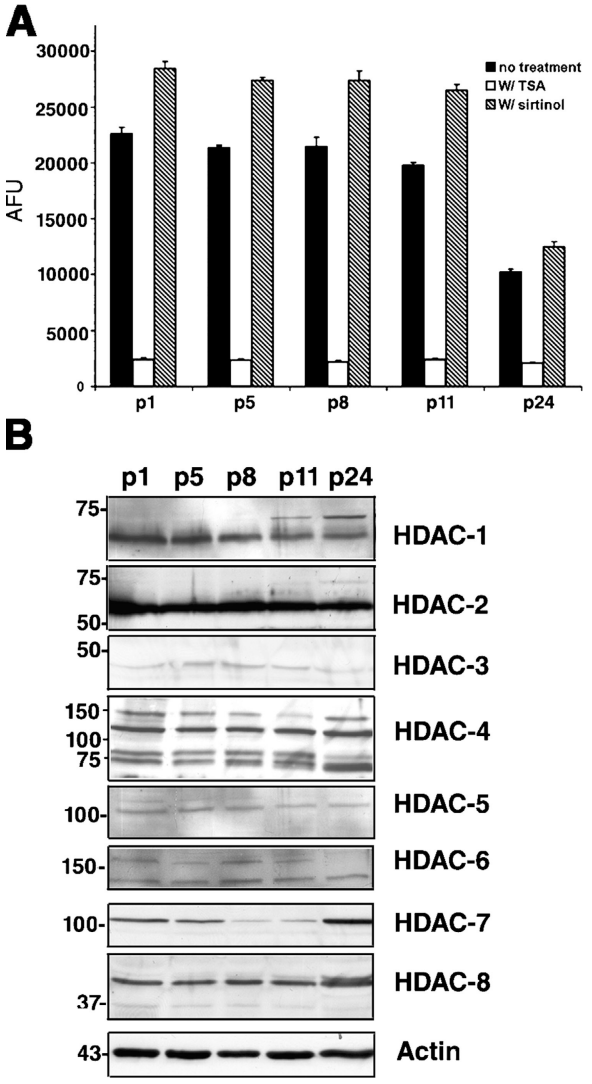

Figure 3. **Total HDAC activity in extracts of the developing rostral corpus callosum.** (A) Total HDAC activity was measured in protein extracts from anterior corpus callosum at p1, p5, p8, p11, and p24 using an acetylated fluorimetric substrate (black bars). The experiments were then repeated by incubating the same samples with TSA (white bars), or with sirtinol (hatched bars). (B) The protein levels of distinct HDAC isoforms were assessed by Western blot analysis on the same tissue extracts. Blots were probed with antibodies against class I (HDAC-1, -2, -3, and -8) and class II (HDAC-4, -5, -6, and -7), and actin as loading control.

CC1 and AcH3 staining (Fig. 2, H–M) and counted the number of double-positive cells. At p5, the total number of CC1+/AcH3+ cells was 716 ± 29 per mm^2 ($n = 3$), whereas at p24 this number was reduced to 234 ± 29 per mm^2 ($n = 3$), thus resulting in a 40% decrease in the number of double-positive cells (Fig. 2 N). Together, these data suggest that progressive deacetylation of histone H3 occurs in cells of the OL lineage, during a critical temporal window coincident with timing of OL differentiation and myelin gene expression in the developing corpus callosum.

Decreased protein acetylation is due to the activity of class I HDACs

Because deacetylation is due to the removal of acetyl groups from lysine residues mediated by specific enzymes called HDACs, we tested the HDAC enzymatic activity in protein extracts from the developing corpus callosum, using a fluorimetric assay (Fig. 3 A). High levels of HDAC activity were detected during the first two weeks of postnatal development and progressively decreased during the third postnatal week (Fig. 3 A). Because the acetylation level of proteins at any time point reflects the equilibrium between the addition and the removal of acetyl groups (Lehrmann et al., 2002), these data suggest that at p1, despite the high levels of HDAC activity, the equilibrium is in favor of acetylation, whereas starting from p5 it is in favor of deacetylation. To determine the class of HDAC responsible for the effect, the experiments were repeated in the presence of the class I and II HDAC inhibitor trichostatin A (TSA), and of the class III HDAC inhibitor sirtinol. TSA decreased the total HDAC activity in the tissue extracts of developing corpus callosum of >90% (Fig. 3 A), whereas sirtinol did not block the HDAC enzymatic activity and it actually induced further activation, possibly due to removal of inhibitory acetyl groups regulating class I and II HDACs.

Given the existence of a large number of isoforms for class I and class II HDACs, it was important to determine their expression and functional relevance in the developing corpus callosum. Western blot analysis of protein extracts from the rostral corpus callosum, dissected at distinct developmental time points, revealed the presence of all the HDACs isoforms (Fig. 3 B). No major change in protein expression was observed for HDAC-1 to HDAC-8, whereas HDAC-7 levels decreased around p8 (Fig. 3 B). Interestingly, HDAC-1 and HDAC-8 both showed the presence of additional higher molecular weight bands at p24, possibly resulting from post-translational modifications of these molecules. The temporal and cellular patterns of HDAC expression in the developing corpus callosum were further assessed using double immunohistochemistry with CC1 and antibodies specific for each HDAC isoform (Fig. 4). At p5, the class I isoforms HDAC-1, -2, -3, and to a lesser degree HDAC-8 were expressed in the nucleus of CC1+ cells (Fig. 4, A–C, H). The class II isoforms HDAC-4, -5, -6, and -7, in contrast, were weakly expressed and localized in the cytoplasm (Fig. 4, D–G). HDAC-4 was completely absent from CC1+ cells and its filamentous staining pattern was suggestive of axonal staining or myelinated fibers in the developing corpus callosum (Fig. 4 D). By p24, when myelination had ensued, the immunoreactivity for several HDAC isoforms, including HDAC-2, -3, -5, and -8, decreased in CC1+ cells (Fig. 4, J, K, M, and P). In contrast, HDAC-1 was still expressed in the nucleus of the CC1+ cells as well as in myelinated fibers (Fig. 4 I), HDAC-4 displayed a strong filamentous staining similar to p5 (Fig. 4 L), and HDAC-6 and -7 were still in the cytosol of CC1+ cells (Fig. 4, N and O).

Due to the nuclear localization of class I HDACs in the p5 corpus callosum, we confirmed the cellular specificity of these isoforms by immunolabeling with antibodies specific for oligodendrocytic (i.e., CC1), neuronal (i.e., NeuN), and astrocytic (i.e., GFAP) markers (Fig. 5). The majority of the HDAC-1–positive cells were identified as OLs because they were immunoreactive predominantly for CC-1 (Fig. 5 A), but not for NeuN (Fig. 5 B) or GFAP (Fig. 5 C). In contrast, a large

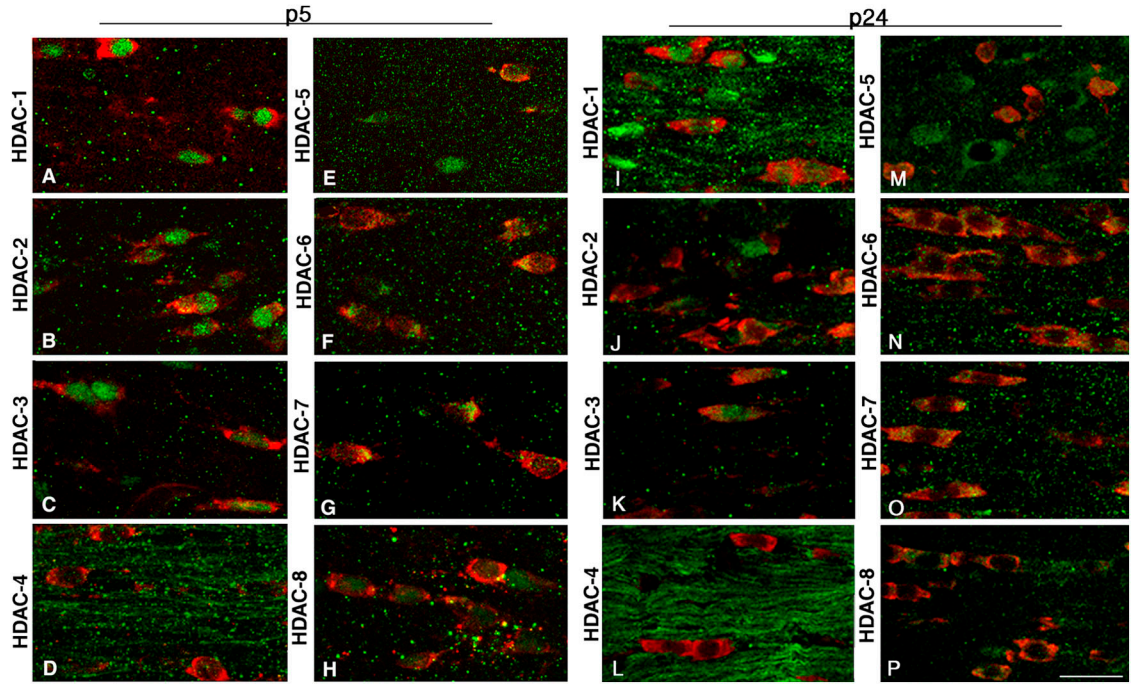

Figure 4. **Cellular and temporal profile of expression of class I and II HDACs in maturing OLs.** Confocal images of the medial part of the body of the corpus callosum at rostral levels, identified in coronal brain sections from p5 (A–H) and p24 (I–P) neonatal rats, after staining with antibodies for HDAC-1 to -8 (A–P, green) and for CC1 (A–P, red). Bar, 20 μm. 63× objective, LSM510 confocal microscope (Carl Zeiss MicroImaging, Inc.).

part of HDAC-2–positive cells were also NeuN+ (Fig. 5 E) and GFAP+ (Fig. 5 F). A similar pattern of expression was observed for HDAC-3 (Fig. 5, G–I) and HDAC-8 (Fig. 5, J–L), which were both expressed in all three cell types.

Together, these data show that during the first week of postnatal development, only class I HDACs are present in the nuclei of the differentiating OL cells, thus suggesting that histone deacetylation in these cells is likely due to the activity of class I HDAC isoforms.

Inhibiton of HDAC activity prevents myelin gene expression in the developing corpus callosum only during a critical temporal window

To address the functional relevance of histone deacetylation on OL differentiation and myelination, we investigated the effect of in vivo administration of the pharmacological inhibitor of class I HDACs, valproic acid (VPA). The short-term experimental paradigm included three groups of neonatal pups receiving a 2-d regimen of VPA (300 mg/kg body weight) starting at distinct developmental time points (Fig. 6 A). The first group of neonatal rats ($n = 12$) was injected with PBS ($n = 6$) or VPA ($n = 6$) at p6 and p7 and then harvested at p8 (injection 1), at the beginning of myelination. The second group ($n = 12$) was injected at p9 and 10 and harvested at p11 (injection 2), whereas the third group ($n = 12$) was injected at p19 and 20 and harvested at p21 (injection 3), after myelination had ensued in the rostral corpus callosum.

The hypothesis that HDAC activity was required for changes in gene expression associated with OL differentiation

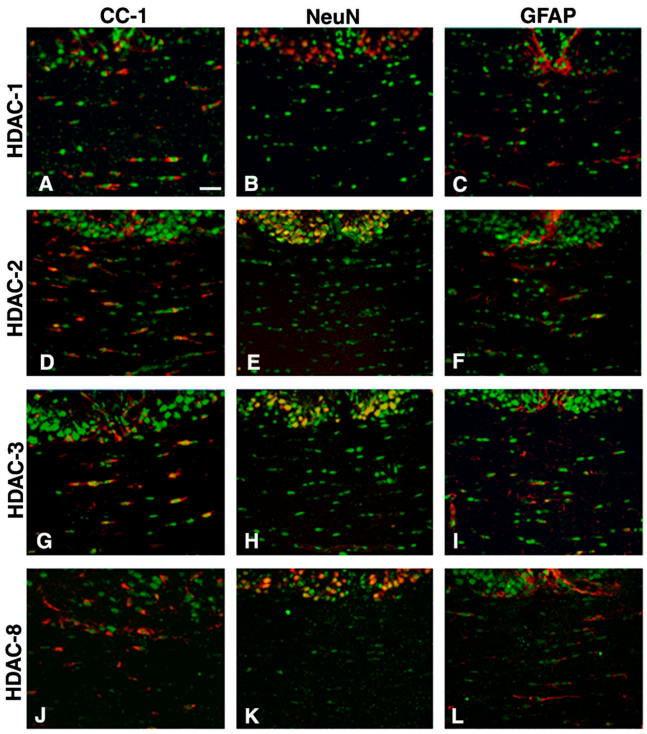

Figure 5. **Cell specificity of class I HDAC expression during the first postnatal week of development.** Immunohistochemistry of coronal brain sections from p5 rat pups stained with antibodies against HDAC-1, -2, -3, and -8 (A–L, green), CC1 (A, D, G, and J, red), NeuN (B, E, H, and K, red), and GFAP (C, F, I, and L, red). Bar, 20 μm. 25× objective, DM RA (Leica). Each immunostaining was performed at least three times from three distinct p5 rat brains.

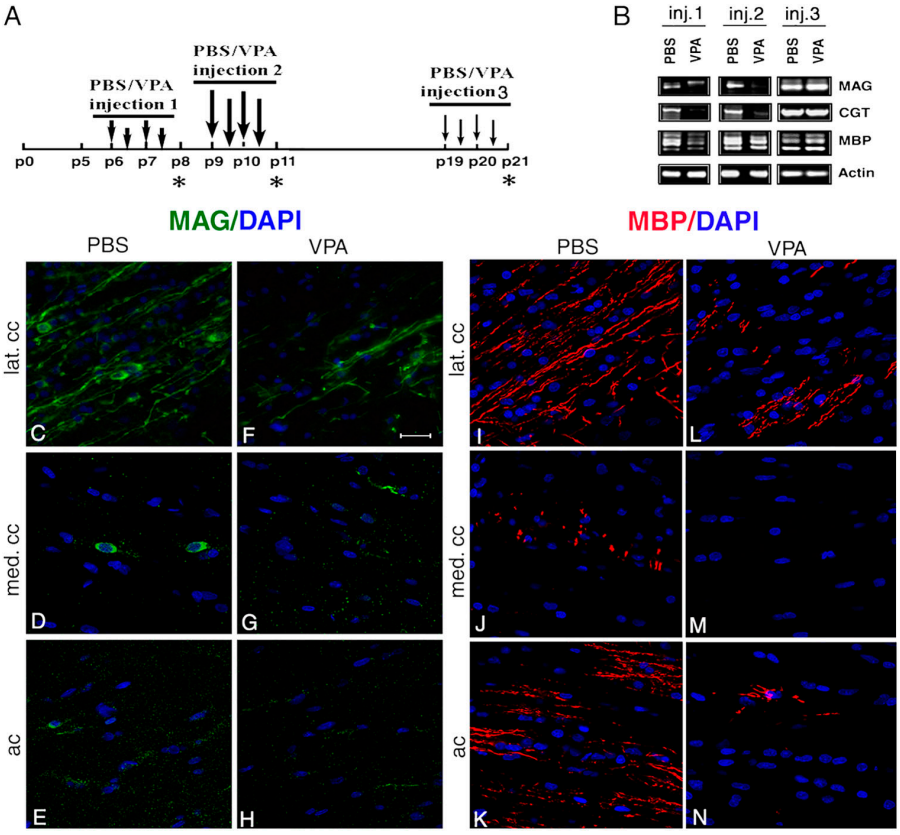

Figure 6. **Pharmacological blockers of HDAC activity induced hypomyelination when administered during a critical temporal window of development.** (A) Schematic representation of three distinct PBS/VPA injection paradigms to the neonatal rats. Each group was composed of 12 animals, receiving four injections (arrows) of either PBS ($n = 6$) or VPA ($n = 6$) at the indicated times. Harvest time is indicated by the asterisk. (B) Semi-quantitative RT-PCR analysis of the effect of the three treatments on myelin gene expressions. Total RNA was isolated at each time point (3 PBS- and 3 VPA-injected pups), and the reverse-transcribed cDNA was amplified using primers specific to MAG, CGT, and MBP, and actin as loading control. (C–N) MAG+ immunofluorescence in control animals was detected in the soma of OL and in myelinated fibers in the lateral corpus callosum (C, lat. cc, green), in the soma of OL in the medial corpus callosum (D, med. cc, green), and in the anterior commissure (E, ac, green). Fewer MAG+ cells and myelinated fibers were detected in the lateral (F) and medial (G) corpus callosum, and in the anterior commissure (H) of VPA-injected rats. (I–N) The pattern of MBP immunofluorescence was similar and showed several myelinated fibers in the lateral corpus callosum (I) and in the anterior commissure (K) of control rats and very few MBP+ fibers in the same brain regions of VPA-treated animals (L–N). Bar, 20 μm. 63× objective, LSM510 confocal microscope (Carl Zeiss MicroImaging, Inc.).

predicted that in vivo treatment with HDAC inhibitors prevented OL differentiation and possibly caused hypomyelination of axonal fibers in the developing corpus callosum. In agreement with this hypothesis, the expression of OL differentiation genes was significantly down-regulated in animals that received VPA injection during the first two postnatal weeks (Fig. 6 B). The effect of VPA on myelin gene expression was dramatic if started during the first postnatal week, but it was ineffective if started during the third postnatal week (Fig. 6 B). Decreased myelin gene expression in the VPA-treated pups was associated with a decreased number of mature OL and myelinated fibers, as assessed by MAG and MBP immunoreactivity. In PBS-injected pups at p8, myelination in the corpus callosum followed the latero-medial gradient, as assessed by the large number of MAG+ and MBP+ cells and fiber in the lateral (Fig. 6, C and I) but not in the medial (Fig. 6, D and J) region. Several myelinated fibers could also be detected in the anterior commissure (Fig. 6, E and K). In VPA-injected pups, in contrast, the number of MAG+ and MBP+ cells and fibers was decreased both in the lateral (Fig. 6, F and L) and medial (Fig. 6, G and M) corpus callosum as well as in the anterior commissure (Fig. 6, H and N).

Decreased MAG and MBP immunoreactivity in the corpus callosum of VPA-treated pups was accompanied by a reduction in the number of CC1+ cells (Fig. 7, A–E). This decrease was not due to a toxic effect of the pharmacological inhibitor because the total number of DAPI+ cells/mm^2 was quite stable ($x = 1488 \pm 49$ in VPA injected and $x = 1563 \pm 52$ in PBS control) and because there was no difference in the number of TUNEL+ (unpublished data) apoptotic cells in the two groups. The reduced number of CC1+ cells was likely due to delayed differentiation, as indicated by the increased percentage of cells expressing the bipotential progenitor marker NG2+ in VPA-treated animals compared with controls (Fig. 7, F–H). The increased progenitor number was not due to an effect of VPA on proliferation, because the number of proliferating NG2+ cells, identified by in vivo labeling with the thymidine analogue BrdU, was very similar in treated and control rats (Fig. 7, I–M). The inhibitory effect of VPA on differentiation was also supported by the detection of PSA-NCAM+ precursors in cells in the subcortical white matter of treated animals (Fig. 7, N–Q). Together, these data suggest that short-term inhibition of HDAC activity does not impair the ability of OL progenitors to exit the cell cycle, but arrests their differentiation at a stage characterized by the expression of early progenitor traits and lack of differentiation markers.

Because a 3-d VPA treatment resulted in hypomyelination, we asked whether prolonged treatment would inhibit myelination even more. To test this hypothesis, pups were subject to a 7-d injection protocol (Fig. 8 A) starting at p3 and followed by the assessment of myelination at p10 (Fig. 8, B–M). In p10 control animals myelination was almost complete in the lateral region of the anterior corpus callosum (Fig. 8, B and H) and in the anterior commissure (Fig. 8, D and J), as indicated by the presence of several CC1+ and MAG+ cells and by the intense MAG and MBP immunoreactivity of the myelinated fibers. At p10 OL differentiation and myelination were detected also in

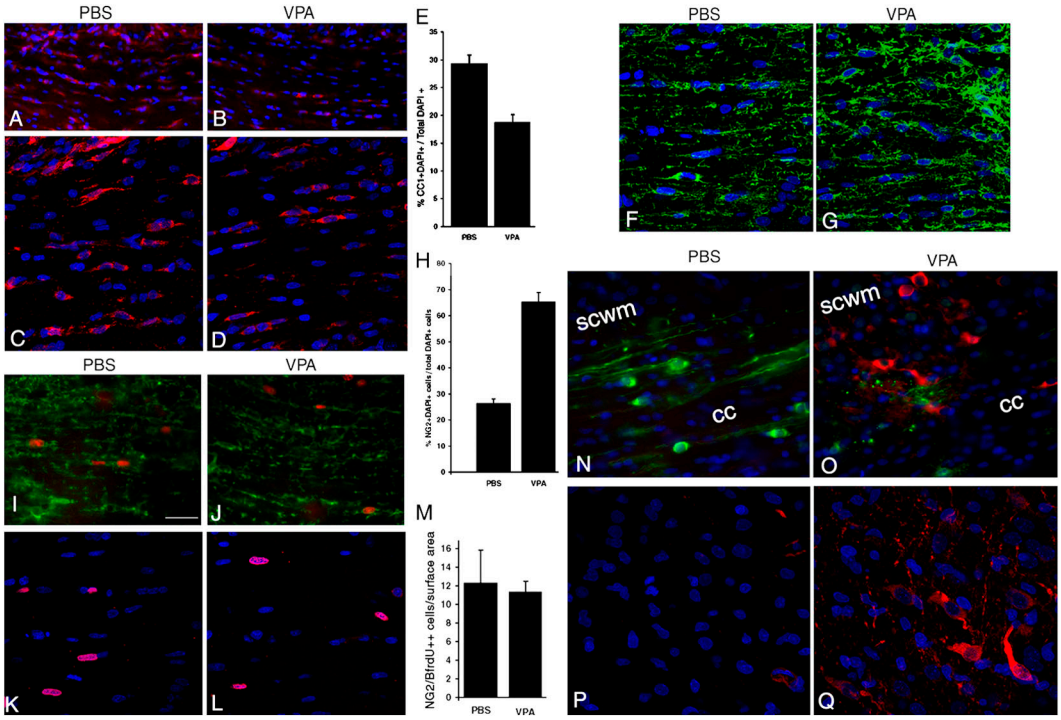

Figure 7. **Hypomyelination in VPA-treated rats resulted from delayed differentiation of OL progenitors.** Coronal brain sections from PBS- (A and C) and VPA (B and D) -injected rats (inj1) were processed for immunohistochemistry using antibodies for CC1 (A and D, red) and DAPI as nuclear counterstain. The number of CC1+ cells was referred to as a percentage of the total DAPI + nuclei (E) and was statistically different in the two treatment groups ($P < 0.01$). The decreased number of CC1+ cells was paralleled by an increased number of OL progenitors identified by the surface marker NG2 (F and G, green). The number of NG2+ cells per total DAPI+ cells in PBS- and VPA-treated rat corpus callosum showed a statistically significant difference ($P < 0.001$) (H). (I–M) The increased number of progenitors was not due to impaired exit from the cell cycle. Cells in the S phase of the cell cycle were labeled in vivo and then identified by immunofluorescence for BrdU (I–L, red) and for NG2 (I and J, green). The number of NG2+/BrdU+ cells (M) was not significantly different between the two groups ($P > 0.5$). (N–Q) The subcortical white matter (scwm) and the corpus callosum (cc) of PBS- (N and P) or VPA (O and Q) -injected rat brains were double stained with antibodies for MAG (N and O, green) and for PSA-NCAM (O and Q, red). Bar in A, B, I, and J = 100 μm. 32× objective, DM RA (Leica). Bar in K–L, 20 μm. 63× objective, LSM510 microscope (Carl Zeiss MicroImaging, Inc.).

the medial corpus callosum (Fig. 8, C and I) of PBS-injected pups. The effect of long-term VPA treatment on myelination was striking. Very few, sparse CC1+ cells and MAG+ and MBP+ fibers were detected in the lateral corpus callosum (Fig. 8, E and K), but not in the medial corpus callosum (Fig. 8, F and L) and in the anterior commissure (Fig. 8, G and M), thus suggesting that longer suppression of HDAC activity led to more severe hypomyelination.

To determine whether the delayed timing of OL differentiation caused by VPA treatment was reversible, we assessed OL differentiation after a recovery period. As expected from a reversible inhibitor, 2 d after the interruption of VPA treatment the OL lineage cells were able to resume the age-appropriate developmental pattern of gene expression characterized by decreased progenitor traits (i.e., Notch1, nestin, and tenascin), increased levels of the transcriptional activator Sox10, and of the late differentiation markers MAG and MBP (Fig. 9 A). The majority of the cells in the corpus callosum of VPA-treated animals after recovery were immunoreactive for CC1 (Fig. 9 G) and MAG (Fig. 9 I). However, few myelinated fibers could be detected in the lateral corpus callosum of VPA-injected animals (Fig. 9, C and I) compared with the more extensive myelination observed in PBS-injected controls (Fig. 9, B and H).

Together, these data support the hypothesis that epigenetic regulation of gene expression is critical for timely differentiation of OLs in the developing corpus callosum.

After myelination onset, cells in the developing corpus callosum acquire more permanent changes in chromatin components and this renders them refractory to the effect of HDAC inhibitors

We have previously discussed that the effectiveness of VPA administration on modulating myelin gene expression in vivo was limited to a specific temporal window coincident with the onset of myelination. To understand the molecular mechanisms defining this developmental window regulated by HDAC activity, we assessed the presence of AcH3 after each protocol of VPA injection (Fig. 10 A). Administration of VPA during the first two postnatal weeks increased the levels of AcH3 without significantly affecting the acetylation state of other high molecular weight proteins (Fig. 10 A). In contrast, administration of VPA during the third postnatal week did not affect the levels of AcH3 (Fig. 10 A). Because protein acetylation is the result of the equilibrium between histone acetyltransferases (i.e., HATs, such as p300 and CBP) and HDACs

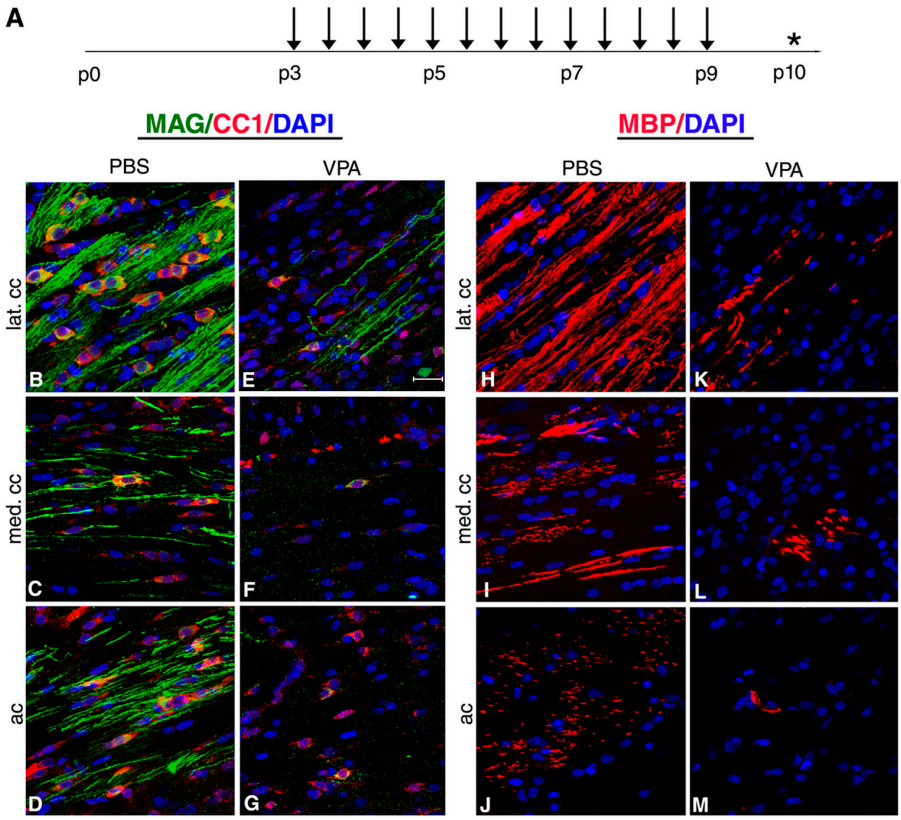

Figure 8. **Long-term treatment with HDAC inhibitors dramatically decreases myelination in the corpus callosum and anterior commissure of the developing rat.** (A) Schematic representation of the long-term PBS/VPA treatment to neonatal rats. Each group was composed of 12 animals, receiving 13 injections (arrows) of either PBS ($n = 6$) or VPA ($n = 6$) at the indicated times. Tissue was harvested on p10 (asterisk). Note that in control rats, several OL were labeled by CC1 (B–D, red) and the majority of fibers in the lateral corpus callosum (B and H) and anterior commissure (D) were myelinated, as indicated by the intense immunoreactivity for MAG (B–G, green) and MBP (H–M, red). In VPA-treated rats, only very few cells expressed CC1 (E–G, red) and the majority of the fibers were not myelinated, as shown by the lack of MAG (E–G, green) and MBP (K–M, red) immunofluorescence. DAPI (B–M, blue) was used as nuclear counterstain. Bar, 20 μm. 63× objective, LSM510 microscope (Carl Zeiss MicroImaging, Inc.).

(Lehrmann et al., 2002; Rouaux et al., 2003), we hypothesized that the lack of VPA in the third postnatal week was consequent to low levels of HATs. This hypothesis was confirmed by the detection of decreased protein levels of CBP and p300 during the third postnatal week of development (Fig. 10 B). The results obtained at p24 suggested that perhaps reversible acetylation was a mechanism of regulation of gene expression that was best suited to maintain a certain "plasticity" of gene expression during early developmental stages. At later developmental stages, however, it was likely that committed cells would adopt more stable mechanisms of regulation of gene expression that would guarantee the maintenance of the differentiated phenotype. Because histone deacetylation is often followed by the more stable methylation of lysine 9 in histone H3 (Honda et al., 1975; Eberharter and Becker, 2002; Boulias and Talianidis, 2004), we asked whether in the corpus callosum the global changes in gene expression initiated by histone deacetylation were also maintained by histone methylation and chromatin compaction. To test this possibility, we stained p5 and p24 brain sections with antibodies specific for methylated histone H3 and for HP1 α, a protein that specifically binds to methylated lysine 9 on histone H3 (MeK9H3) and identifies the presence of compact chromatin (Bannister et al., 2001; Lachner et al., 2001). In agreement with our hypothesis, at p5 before the peak of myelination, OL progenitors did not show MeK9H3+ or HP1α immunoreactivity (Fig. 10, C–F). In contrast, by p24 the majority of the cells in the corpus callosum were MeK9H3+/HP-1 α+ (Fig. 10, G–J), thus confirming the acquisition of compact chromatin structure.

Together, these data indicate that HDAC activity is critical during the first two weeks of postnatal development of the corpus callosum and is associated with the reversible modulation of gene expression at the onset of myelination. During the third postnatal week, however, after myelination has ensued, this reversible form of regulation of gene expression is replaced by more stable changes resulting in chromatin compaction.

Discussion

The process of myelination in the developing corpus callosum has been well characterized. It is clearly established that expression of myelin components begins during the first two postnatal weeks of development (Bjelke and Seiger, 1989; Bjartmar et al., 1994; Hamano et al., 1996, 1998), but still relatively little is known about the molecular mechanisms underlying this event. We and others have previously reported that myelination is a complex phenomenon, requiring the regulated expression of positive and negative modulators of OL differentiation (Kondo and Raff, 2000a,b; Wang et al., 2001; Marin-Husstege et al., 2002; Stolt et al., 2002; Liu et al., 2003).

We now show that deacetylation of histone H3 is a critical mechanism for myelination onset in vivo because it is required for the down-regulation of differentiation inhibitors and early progenitor markers. Administration of the HDAC inhibitor VPA during the critical period of myelination onset inhibited the progression of OL progenitors along the lineage. This arrest in differentiation was characterized by timely exit from

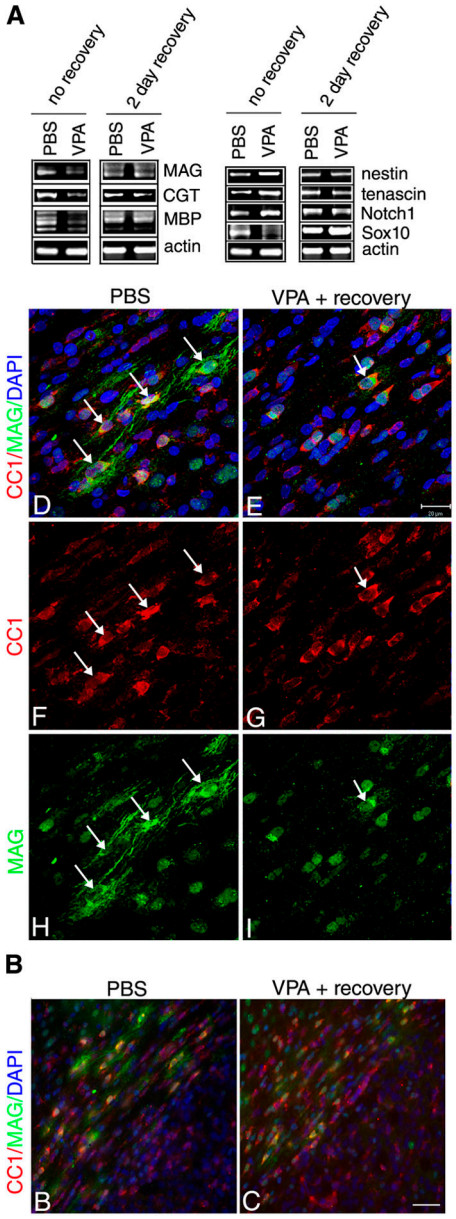

Figure 9. **The inhibitory effect of VPA on OL differentiation was reversible.** (A) To address whether OL differentiation was delayed or irreversibly impaired by VPA treatment, we repeated protocol 1 with a recovery period of 3 d after the last injection. At p11 RNA was extracted, and the myelin gene expression and the presence of inhibitors were assessed by semi-quantitative RT-PCR. (B and C) Micrographs of coronal brain sections stained for CC1 (red), MAG (green), and DAPI (blue). Bar, 100 μm. 32× objective, DM RA (Leica). (D–I) Confocal images of the lateral corpus callosum of PBS- or VPA-injected rats after 2 d of recovery. Although extensive myelination was observed in PBS-treated controls (D, F, and H, white arrows), the majority of cells in the VPA-treated animals were CC1, but only few of them had started to myelinate (E, G, and I, white arrow). Bar, 20 μm. 63× objective, LSM510 microscope (Carl Zeiss MicroImaging, Inc.).

the cell cycle, persistence of progenitor traits and lack of late differentiation markers, thereby identifying histone deacetylation as the molecular link of the transition between cell cycle exit and differentiation onset.

Deacetylation of histone H3 during myelination onset was attributed to class I HDACs. The HDAC enzymatic activity in tissue extracts was selectively inhibited by the inhibitor TSA but not by the class III inhibitor sirtinol, and only the class I isoforms (HDAC-1, -2, -3, and -8) showed nuclear localization. Interestingly, HDAC-1 was predominantly detected in OL lineage cells throughout development, whereas HDAC-2, -3, and -8 were also found in neurons and astrocytes. Therefore class I HDACs were likely to be responsible for the removal of acetyl groups from histone H3 in OL lineage cells, whereas class II HDACs played a role in modulating acetylation of cytosolic substrates

Histone acetylation was previously shown to result from a balance between the addition (by HATs) and the removal (by HDACs) of acetyl group on specific lysine residues (Lehrmann et al., 2002; Rouaux et al., 2003) and to result in a transcriptionally active chromatin conformation (Eberharter and Becker, 2002), thus implying this secondary modification of histone as a reversible switch regulating gene expression. In agreement with this concept, HDAC inhibition in VPA-treated rats created a disequilibrium characterized by the predominance of HAT activity. The resulting increase of H3 acetylation was functionally associated with high levels of differentiation inhibitors and with the persistence of progenitor traits. Due to the reversible nature of this secondary modification of histone H3, we anticipated that upon interruption of VPA treatment the animals would resume a normal pattern of myelination. Consistent with this hypothesis, after only two days of recovery, progenitors rapidly down-regulated the inhibitors, up-regulated transcriptional activators, and expressed OL markers such as CC1 and MAG. In addition, some of the newly generated OL started to myelinate the callosal axons, as indicated by the presence of MAG immunoreactive fibers. These data support the idea that HDAC activity is necessary for the repression of genes inhibiting differentiation and are in agreement with results recently obtained in zebrafish (Cunliffe, 2004).

Our study also has important clinical implications because it suggests that treatment with VPA, a pharmacological agent currently used in the management of seizures, can negatively affect myelination in the corpus callosum if delivered during a critical temporal window of development. The inhibitory effect of VPA on myelination was observed only if the administration occurred during the first two postnatal weeks. At later time points, VPA administration did not affect myelin gene expression and OL differentiation, thus suggesting the existence of alternative mechanism of regulation of gene expression, occurring at later developmental stages. It has been reported that histone deacetylation is often followed by the more stable histone methylation (Eberharter and Becker, 2002; Boulias and Talianidis, 2004). Indeed, we demonstrated that the reversible deacetylation of lysine residues on histone H3—observed in cells of the OL lineage during the first two weeks of development—was later replaced by the more stable methylation of lysine 9 in histone H3 and by the expression of the HP1 α protein, a marker of chromatin compaction. Therefore, our results identified histone acetylation as a reversible mechanism regulating the expression of progenitor traits during early developmental stages, when progenitors showed a certain degree of "plasticity." At later developmental stages, however, the committed cells adopted more

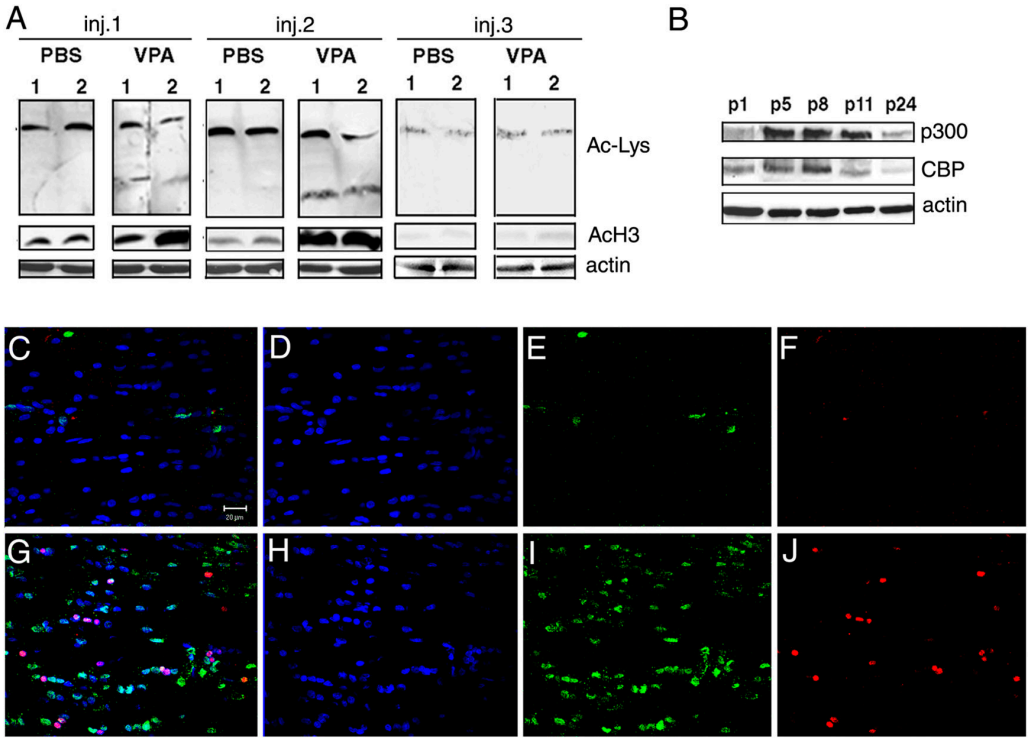

Figure 10. **Global histone deacetylation occurred only during the first two weeks of postnatal development and was followed by histone methylation and chromatin compaction.** (A) To confirm the inhibitory effect of VPA, Western blot analysis was performed on total proteins extracted from the corpus callosum of injected rats using antibody for AcLys. The increased acetylated 14-kD band was confirmed to be histone H3 by using antibody for AcH3. At p21, VPA injection did not increase histone H3 acetylation. (B) Western blot analysis of total protein extracted from the body of developing corpus callosum at anterior levels at the indicated time points. The blots were probed with antibodies for the HATs CBP and p300, and actin was used as loading control. (C–J) Immunofluorescence on cryosections using antibodies specific for methylated lysine 9 on histone H3 (MeK9H3; C, E, G, and I, green) and for HP1 α (C, F, G, and J, red). Co-expression of HP1α and MeK9H3 in p24 corpus callosum reveals the establishment of a compact chromatin structure at later stages of OL differentiation. Bar, 20 μm. 63× objective, LSM510 microscope (Carl Zeiss MicroImaging, Inc.).

stable mechanisms of repression, dependent on histone methylation and HP1 α binding. These changes defined the acquisition of compacted chromatin associated with decreased levels of differentiation inhibitors possibly to favor the maintenance of the differentiated phenotype.

The progressive compaction of chromatin during OL development was consistent with morphological studies on the ultrastructure of developing OL in the corpus callosum of neonatal rats (Mori and Leblond, 1970; Kozik, 1976; Sturrock, 1976). According to these studies, at p1 progenitors were identified by the presence of a pale nucleus with dispersed chromatin and abundant cytoplasm (Mori and Leblond, 1970; Sturrock, 1976). At p8 the appearance of the differentiating cells, called "oligodendroblasts," was characterized by a slightly higher electron density and by the presence of large conglomerates of nuclear chromatin in the inner part of the nuclear membrane (Kozik, 1976). Finally, around the third week of postnatal development, the nucleus of OL was characterized by the presence of very large chromatin aggregates and smaller granules scattered throughout (Mori and Leblond, 1970; Kozik, 1976; Sturrock, 1976). Our data provide a molecular explanation to this very well-characterized morphological profile because histone acetylation was consistent with the dispersed chromatin observed in progenitor cells, histone deacetylation correlated with the initiation of chromatin compaction observed around p8, and finally, histone methylation and HP1 α binding were observed coincident with the report of chromatin condensation in mature OL.

In conclusion, this study provides evidence that epigenetic regulation of gene expression in cells of the OL lineage modulates timing of OL differentiation in the developing corpus callosum. Although the appearance of nuclear chromatin in the corpus callosum is a well-established ultrastructural criterion for identification of cells from the OL lineage (Mori and Leblond, 1970; Kozik, 1976; Sturrock, 1976; Imamoto et al., 1978), the functional relevance of chromatin compaction in progenitor differentiation has never been investigated. In this manuscript we describe the mechanisms responsible for the progressive compaction of chromatin observed during the maturation of progenitor cells into myelinating OLs. Further, we identify the biological significance of post-translational modifications of nucleosomal histones as a global event responsible for timing of OL differentiation and myelination of the developing corpus callosum.

Materials and methods

Antibodies

HDAC1 (1:6,000 for IHC, 1:4,000 for WB; Affinity BioReagents, Inc.); HDAC2 (1:100 for IHC, 1:1,000 for WB; Santa Cruz Biotechnology, Inc.); HDAC3 (1:100 for IHC, 1:500 for WB; Santa Cruz Biotechnology, Inc.);

HDAC4 (1:100 for IHC, 1:1,000 for WB; Upstate Biotechnology); HDAC5 (1:100 for IHC, 1:500 for WB; Santa Cruz Biotechnology, Inc.); HDAC6 (1:100 for IHC, 1:500 for WB; Santa Cruz Biotechnology, Inc.); HDAC7 (1:100 for IHC, 1:500 for WB; Santa Cruz Biotechnology, Inc.); HDAC8 (1:100 for IHC, 1:500 for WB; Santa Cruz Biotechnology, Inc.); acetylated-lysine (1:1,000 for IHC and WB; Upstate Biotechnology); acetylated H3 (1:10,000 for IHC and 1:1,000 for WB; Upstate Biotechnology); di-methylated H3 (1:100 for IHC; Upstate Biotechnology); actin (1:1,000 for WB; Sigma-Aldrich); APC/CC1 (1:50 for IHC; Oncogene Research Products); Sox10 (1:400 for IHC; a gift from Dr. M. Wagner, Universität Erlangen-Nürnberg, Germany); NG2 chondroitin sulfate proteoglycan (1:200 for IHC; CHEMICON International); CBP (1:1,000 for WB; Santa Cruz Biotechnology, Inc.); p300 (1:500 for WB; Santa Cruz Biotechnology, Inc.); HP1-α (1:500 for IHC; CHEMICON International); S/L MAG (1:200 for IHC; Zymed Laboratories); MBP (1:1,000; Sternberger Monoclonals, Inc.); and BrdU (1:100 for IHC; DakoCytomation).

PBS/VPA injection

The first group of neonatal pups subject to subcutaneous injection (injection protocol 1) consisted of p6 animals injected either with PBS ($n = 6$) or with VPA (300 mg/kg weight; $n = 6$). Each animal received a total of four injections, administered every 12 h for two consecutive days. Injected rats were then either killed on p8 and the brain tissues were dissected out and subject to total RNA extraction or protein lysis, or perfused with 4% PFA for coronal cryosections. The second group of neonatal pups (injection protocol 2), consisting of p9 animals, was subject to subcutaneous injection of PBS ($n = 6$) or VPA ($n = 6$), repeated every 12 h for 4 times, and was followed by tissue harvesting at p11. Brain tissue from these injected rats was subject to total RNA extraction or protein lysis. The third group (injection protocol 3), consisting of p19 pups, received subcutaneous injection of PBS ($n = 6$) or VPA ($n = 6$) every 12 h for 4 times followed by harvesting on p21. The anterior portion of the corpus callosum surrounding the bregma was carefully dissected and the extracted proteins were processed for Western blot analysis. The fourth group (injection protocol 4), consisting of p3 pups, received a subcutaneous injection of PBS ($n = 6$) or VPA ($n = 6$) every 12 h for 4 times, followed by tissue harvesting on p5. The long-term treatment consisted of 13 injections from p3 to p10. The toxicity of the treatment was monitored by daily recording of the body weight. For the recovery experiments, neonatal rats received the injections as described in protocol 1 and 4 ($n = 6$ for PBS and $n = 6$ for VPA), followed by a recovery period of three days before sacrifice.

Immunohistochemistry and analysis of corpus callosum and anterior commissure

Untreated neonatal rats (p1, p5, p8, p11, and p24) and PBS- or VPA-injected neonatal rats (see injection protocols) were anesthetized and then perfused with 4% PFA in 0.1 M phosphate buffer. The whole brains were removed from the skulls, post-fixed, then cryopreserved in 30% sucrose, embedded in OCT and sectioned coronally (20 μm). Frozen sections were first permeabilized with blocking buffer (0.1 M phosphate buffer, 5% normal goat serum [Vector Laboratories], and 0.5% Triton X-100). Note that for better staining with HDACs it was necessary to process the sections for antigen retrieval by incubation in citrate buffer (Poly Scientific), pH 6.8, at 65°C for 2 h before the blocking step. Incubation with primary antibodies against HDACs, myelin proteins, or other lineage progression markers was performed overnight at RT (see Antibodies section for sources and dilutions). The following day, after 1 h incubation with secondary antibodies, either directly conjugated to specific fluorochromes (whole Ig-Cy3, 1:200; Sigma-Aldrich) or biotinylated (RPN-1004, 1:200; Amersham Biosciences), the sections were counterstained with DAPI (1:1,000; Molecular Probes, Inc.) in the absence or presence of avidin-conjugated FITC or Texas red (RPN-1232 and RPN-1233, diluted 1:500; Amersham Biosciences). Stained sections were visualized using an inverted fluorescence microscope (DM RA; Leica) and confocal microscopy (LSM510 Meta confocal laser scanning microscope; Carl Zeiss MicroImaging, Inc.). The immunohistochemical analysis on the rostral corpus callosum at p5 was conducted on coronal sections corresponding to plates 155–160 of the p0 images of the "Atlas of the Developing Rat Nervous System" (Paxinos et al., 1994), upon adjustments of the distance from bregma to lambda at p0 to the measured distance between these two sutures at p5. The anterior commissure was analyzed in sections corresponding to plates 156 and 157 of the same atlas (Paxinos et al., 1994). The immunohistochemical analysis of the anterior portion of the body of the corpus callosum at p24 was conducted posterior to the genu, on coronal sections corresponding to plates 15–19 of the atlas "The Rat Brain in Stereotaxic Coordinates" (Paxinos and Watson, 1986). The anterior commissure was analyzed in coronal brain sections corresponding to plates 18 and 19 of the same atlas (Paxinos and Watson, 1986). The "medial corpus callosum" was defined as the region corresponding to −1 L, +1R of the same atlases. For the functional studies on PBS- or VPA-injected rats of different neonatal ages, the rostral corpus callosum and the anterior commissure were analyzed using similar criteria, adjusting the Atlas to the exact bregma to lambda distance at each developmental age (Paxinos and Watson, 1986; Paxinos et al., 1994).

Western blot analysis

Upon carefully removing the skin over the skull, the positions of the bregma and lambda sutures were marked on the brain surface. These positions were used as a reference point in dissecting out the same regions of corpus callosum from rats of different developing stages. A coronal slice around the bregma was dissected out, and the corpus callosum was excised under a dissection microscope (Nikon) and used for either protein or RNA extraction. Tissue lysates from freshly dissected corpus callosum were prepared by digestion in a buffer containing 50 mM Hepes, pH 7.0, 250 mM NaCl, 0.15% Nonidet P-40, 1 mM DTT, 1 mM EDTA, 0.01% PMSF, 1 mM aprotinin, and 1 mM leupeptin for 15 min on ice. This was followed by mechanical disruption via serial passages through a series of syringes equipped with different-sized needles (18G11/2, 22G11/2, and 26G3/8). Cell membranes were further disrupted by sonication on ice at the highest output (twice, 30 s each; cells were kept on ice for 1 min between each pulse). After high speed centrifuge, protein concentration was determined using the Bradford's method (Bio-Rad Laboratories protein assay) and equal amounts (100 μg) were loaded on SDS-PAGE for separation. Transfer of protein onto a 0.22-μm nitrocellulose membrane was conducted using a Bio-Rad Laboratories apparatus at 30 V for 16–18 h in a transfer buffer containing 25 mM Tris base, 192 mM glycine, 20% (vol/vol) methanol, and 0.04% SDS, pH 8.3. Western blot analysis was performed as reported previously (Casaccia-Bonnefil et al., 1997, 1999) using the appropriate dilutions of primary and secondary antibodies (see Antibodies section for details). The immunoreactive bands were detected by ECL Plus Western Blotting Detection System (Amersham Biosciences). Equal protein loading was guaranteed by probing the blots with antibody against actin.

RT-PCR

Total RNA was isolated using RNeasy Mini kit (QIAGEN) from individually dissected rat corpus callosum. Total RNA (9 μg/each sample) was used in 40 μl of reverse transcription reaction. The PCR was performed in a 20-μl reaction mixture containing 2 μl cDNA as template and 0.1 μM specific oligonucleotide primer pair. Cycle parameters were 30 s at 94°C, 30 s at 50°C, and 1.5 min at 72°C for 25 cycles. The following oligonucleotide primers were used: for rat cerebroside-galactosyl transferase (CGT) the forward primer was 5′-GGAGTGCTGTTGGAATAGCAA-3′, and the reverse primer was 5′-CGTACTCCTAGAACACAGACTT-3′; for rat MAG, the forward primer was 5′-CACCTCGAGTCGCCTTTGCCATCCTGATT-3′, and the reverse primer was 5′-TCTCCATGGCCTTGACTCGGATTTCTGCATAC-3′; for rat MBP, the forward primer was 5′-ATGGCATCACAGAAGAGACC-3′, and the reverse primer was 5′-CATGGGAGATCCAGAGCGGC-3′; for rat Sox10, the forward primer was 5′-GGAGCAAGACCTATCAGAGGT-3′, and the reverse primer was 5′-CAAAGGTCTCCATGTTGGACA-3′; for rat Notch-1, the forward primer was 5′-CAACGGCACTGAAGCCTGTGT-3′, and the reverse primer was 5′-GCACAGTCATCAATGTTGTCA-3′; for rat nestin, the forward primer was 5′-TGCAGCCACTGAGGTATCTG-3′, and the reverse primer was 5′-CAGTTCCCACTCCTGTGGTT-3′; for rat tenascin, the forward primer was 5′-AACAGGTCTCAGAGAGGCCA-3′, and the reverse primer was 5′-CTTCTCTGCGGTCTCCAAAC-3′; for rat Jagged-1, the forward primer was 5′-AACAGAACACAGGGATTGCC-3′, and the reverse primer was 5′-CTTGCCCTCGTAGTCCTCAG-3′; for rat actin, the forward primer was 5′-TGGAATCCTGTGGCATCC-3′, and the reverse primer was 5′-TCGTACTCCTGCTTGCTG-3′.

Total HDAC enzymatic activity measurement

HDAC activity was measured by using HDAC Activity Assay/Drug Discovery Kit (BIOMOL Research Laboratories, Inc.). Experimental procedures were designed and performed according to the protocol provided within the kit. In brief, tissue lysates from the rat corpus callosum (prepared according to the same procedure described in Western blot analysis section) were used as sources for HDAC activity. Sample lysates containing 100 μg protein were added to a 96-well plate in 25 μl HDAC assay buffer (BIOMOL Research Laboratories, Inc.). A fluorimetric acetylated substrate was added and the reaction was allowed occurring at RT for 1 h, then incubated with developer for 10–15 min. Enzymatic activity was evaluated in a microtiter

plate–reading fluorimeter (excitation = 360 nm, detection of emitted light = 460 nm). HeLa nuclear extract (KI-140) was used as positive control.

BrdU incorporation in vivo and TUNEL

Neonatal rat pups received 10 mg/Kg BrdU injection 1 h before sacrifice. After perfusion and cryopreservation, brains were sectioned and stained with cellular markers. For immunolabeling with anti-BrdU antibodies, after the completion of the first staining, the cells were then treated with 2N HCl for 10 min at 37°C in order to denature DNA, followed by equilibration in 0.1 M sodium borate, pH 8.6, for 10 min. The primary antibody for anti-BrdU (DakoCytomation) was used at 1:100 dilution in PGBA containing 0.5% Triton X-100 for at least 3 h at RT, followed by Cy3-conjugated whole-Ig secondary antiserum. Cells were then counterstained with DAPI for nuclei visualization. The identification of apoptotic cells was performed using the ApopTag plus kit from CHEMICON International on cryosections, following the manufacturer's instructions.

This work was supported by grants RO1-NS42925 from the National Institute of Neurological Disorders and Stroke (National Institutes of Health) and RG3421-A-4 from the National Multiple Sclerosis Society (to P. Casaccia-Bonnefil).

Submitted: 15 December 2004
Accepted: 18 April 2005

References

Bannister, A.J., P. Zegerman, J.F. Partridge, E.A. Miska, J.O. Thomas, R.C. Allshire, and T. Kouzarides. 2001. Selective recognition of methylated lysine 9 on histone H3 by the HP1 chromo domain. *Nature.* 410:120–124.

Barres, B.A., M.A. Lazar, and M.C. Raff. 1994. A novel role for thyroid hormone, glucocorticoids and retinoic acid in timing oligodendrocyte development. *Development.* 120:1097–1108.

Bjartmar, C., C. Hildebrand, and K. Loinder. 1994. Morphological heterogeneity of rat oligodendrocytes: electron microscopic studies on serial sections. *Glia.* 11:235–244.

Bjelke, B., and A. Seiger. 1989. Morphological distribution of MBP-like immunoreactivity in the brain during development. *Int. J. Dev. Neurosci.* 7:145–164.

Bjerling, P., R.A. Silverstein, G. Thon, A. Caudy, S. Grewal, and K. Ekwall. 2002. Functional divergence between histone deacetylases in fission yeast by distinct cellular localization and in vivo specificity. *Mol. Cell. Biol.* 22:2170–2181.

Boulias, K., and I. Talianidis. 2004. Functional role of G9a-induced histone methylation in small heterodimer partner-mediated transcriptional repression. *Nucleic Acids Res.* 32:6096–6103.

Casaccia-Bonnefil, P., R. Tikoo, H. Kiyokawa, V. Friedrich, M.V. Chao, and A. Koff. 1997. Oligodendrocyte precursor differentiation is perturbed in the absence of the cyclin-dependent kinase inhibitor p27Kip1. *Genes Dev.* 11:2335–2346.

Casaccia-Bonnefil, P., R.J. Hardy, K.K. Teng, J.M. Levine, A. Koff, and M.V. Chao. 1999. Loss of p27Kip1 function results in increased proliferative capacity of oligodendrocyte progenitors but unaltered timing of differentiation. *Development.* 126:4027–4037.

Cunliffe, V.T. 2004. Histone deacetylase 1 is required to repress Notch target gene expression during zebrafish neurogenesis and to maintain the production of motoneurones in response to hedgehog signalling. *Development.* 131:2983–2995.

de Ruijter, A.J., A.H. van Gennip, H.N. Caron, S. Kemp, and A.B. van Kuilenburg. 2003. Histone deacetylases (HDACs): characterization of the classical HDAC family. *Biochem. J.* 370:737–749.

Durand, B., and M. Raff. 2000. A cell-intrinsic timer that operates during oligodendrocyte development. *Bioessays.* 22:64–71.

Durand, B., F.B. Gao, and M. Raff. 1997. Accumulation of the cyclin-dependent kinase inhibitor p27/Kip1 and the timing of oligodendrocyte differentiation. *EMBO J.* 16:306–317.

Durand, B., M.L. Fero, J.M. Roberts, and M.C. Raff. 1998. p27Kip1 alters the response of cells to mitogen and is part of a cell-intrinsic timer that arrests the cell cycle and initiates differentiation. *Curr. Biol.* 8:431–440.

Eberharter, A., and P.B. Becker. 2002. Histone acetylation: a switch between repressive and permissive chromatin. Second in review series on chromatin dynamics. *EMBO Rep.* 3:224–229.

Fischle, W., F. Dequiedt, M.J. Hendzel, M.G. Guenther, M.A. Lazar, W. Voelter, and E. Verdin. 2002. Enzymatic activity associated with class II HDACs is dependent on a multiprotein complex containing HDAC3 and SMRT/N-CoR. *Mol. Cell.* 9:45–57.

Forsberg, E.C., and E.H. Bresnick. 2001. Histone acetylation beyond promoters: long-range acetylation patterns in the chromatin world. *Bioessays.* 23:820–830.

Gottlicher, M. 2004. Valproic acid: an old drug newly discovered as inhibitor of histone deacetylases. *Ann. Hematol.* 83(Suppl 1):S91–S92.

Grozinger, C.M., E.D. Chao, H.E. Blackwell, D. Moazed, and S.L. Schreiber. 2001. Identification of a class of small molecule inhibitors of the sirtuin family of NAD-dependent deacetylases by phenotypic screening. *J. Biol. Chem.* 276:38837–38843.

Gurvich, N., O.M. Tsygankova, J.L. Meinkoth, and P.S. Klein. 2004. Histone deacetylase is a target of valproic acid-mediated cellular differentiation. *Cancer Res.* 64:1079–1086.

Hamano, K., N. Iwasaki, T. Takeya, and H. Takita. 1996. A quantitative analysis of rat central nervous system myelination using the immunohistochemical method for MBP. *Brain Res. Dev. Brain Res.* 93:18–22.

Hamano, K., T. Takeya, N. Iwasaki, J. Nakayama, T. Ohto, and Y. Okada. 1998. A quantitative study of the progress of myelination in the rat central nervous system, using the immunohistochemical method for proteolipid protein. *Brain Res. Dev. Brain Res.* 108:287–293.

Honda, B.M., P.M. Candido, and G.H. Dixon. 1975. Histone methylation. Its occurrence in different cell types and relation to histone H4 metabolism in developing trout testis. *J. Biol. Chem.* 250:8686–8689.

Ibarrola, N., M. Mayer-Proschel, A. Rodriguez-Pena, and M. Noble. 1996. Evidence for the existence of at least two timing mechanisms that contribute to oligodendrocyte generation in vitro. *Dev. Biol.* 180:1–21.

Imamoto, K., J.A. Paterson, and C.P. Leblond. 1978. Radioautographic investigation of gliogenesis in the corpus callosum of young rats. I. Sequential changes in oligodendrocytes. *J. Comp. Neurol.* 180:115–128, 132–137.

Kondo, T., and M. Raff. 2000a. Oligodendrocyte precursor cells reprogrammed to become multipotential CNS stem cells. *Science.* 289:1754–1757.

Kondo, T., and M. Raff. 2000b. The Id4 HLH protein and the timing of oligodendrocyte differentiation. *EMBO J.* 19:1998–2007.

Lachner, M., D. O'Carroll, S. Rea, K. Mechtler, and T. Jenuwein. 2001. Methylation of histone H3 lysine 9 creates a binding site for HP1 proteins. *Nature.* 410:116–120.

Lehrmann, H., L.L. Pritchard, and A. Harel-Bellan. 2002. Histone acetyltransferases and deacetylases in the control of cell proliferation and differentiation. *Adv. Cancer Res.* 86:41–65.

Liu, A., M. Muggironi, M. Marin-Husstege, and P. Casaccia-Bonnefil. 2003. Oligodendrocyte process outgrowth in vitro is modulated by epigenetic regulation of cytoskeletal severing proteins. *Glia.* 44:264–274.

Kozik, M.B. 1976. The electron-microscopic picture of postnatal development of oligodendroglia. *Folia Histochem. Cytochem. (Krakow).* 14:99–106.

Marin-Husstege, M., M. Muggironi M, A. Liu, and P. Casaccia-Bonnefil. 2002. Histone deacetylase activity is necessary for oligodendrocyte lineage progression. *J. Neurosci.* 22:10333–10345.

Mori, S., and C.P. Leblond. 1970. Electron microscopic identification of three classes of oligodendrocytes and a preliminary study of their proliferative activity in the corpus callosum of young rats. *J. Comp. Neurol.* 139:1–28.

Paxinos, G., and C. Watson. 1986. The rat brain in stereotaxic coordinates. 2nd ed. Academic Press, Orlando, FL. 119 pp.

Paxinos, G., K.W.S. Ashwell, and I. Tork. 1994. Atlas of the developing rat nervous system. 2nd ed. Academic Press, San Diego, CA. 218 pp.

Phiel, C.J., F. Zhang, E.Y. Huang, M.G. Guenther, M.A. Lazar, and P.S. Klein. 2001. Histone deacetylase is a direct target of valproic acid, a potent anticonvulsant, mood stabilizer, and teratogen. *J. Biol. Chem.* 276:36734–36741.

Rouaux, C., N. Jokic, C. Mbebi, S. Boutillier, J.P. Loeffler, and A.L. Boutillier. 2003. Critical loss of CBP/p300 histone acetylase activity by caspase-6 during neurodegeneration. *EMBO J.* 22:6537–6549.

Smith, M.E. 1973. A regional survey of myelin development: some compositional and metabolic aspects. *J. Lipid Res.* 14:541–551.

Stolt, C.C., S. Rehberg, M. Ader, P. Lommes, D. Riethmacher, M. Schachner, U. Bartsch, and M. Wegner. 2002. Terminal differentiation of myelin-forming oligodendrocytes depends on the transcription factor Sox10. *Genes Dev.* 16:165–170.

Strahl, B.D., and C.D. Allis. 2000. The language of covalent histone modifications. *Nature.* 403:41–45.

Sturrock, R.R. 1976. Light microscopic identification of immature glial cells in semithin sections of the developing mouse corpus callosum. *J. Anat.* 122:521–537.

Tang, D.G., Y.M. Tokumoto, and M.C. Raff. 2000. Long-term culture of purified postnatal oligodendrocyte precursor cells. Evidence for an intrinsic maturation program that plays out over months. *J. Cell Biol.* 148:971–984.

Temple, S., and M.C. Raff. 1986. Clonal analysis of oligodendrocyte development in culture: evidence for a developmental clock that counts cell divisions. *Cell.* 44:773–779.

Tikoo, R., D.J. Osterhout, P. Casaccia-Bonnefil, P. Seth, A. Koff, and M.V. Chao. 1998. Ectopic expression of p27Kip1 in oligodendrocyte progenitor cells results in cell-cycle growth arrest. *J. Neurobiol.* 36:431–440.

Turner, B.M. 2000. Histone acetylation and an epigenetic code. *Bioessays.* 22:836–845.

Wade, P.A. 2001. Transcriptional control at regulatory checkpoints by histone deacetylases: molecular connections between cancer and chromatin. *Hum. Mol. Genet.* 10:693–698.

Wang, S., A. Sdrulla, J.E. Johnson, Y. Yokota, and B.A. Barres. 2001. A role for the helix-loop-helix protein Id2 in the control of oligodendrocyte development. *Neuron.* 29:603–614.

Yang, X.J. 2004. Lysine acetylation and the bromodomain: a new partnership for signaling. *Bioessays.* 26:1076–1087.

Yoshida, M., T. Shimazu, and A. Matsuyama. 2003. Protein deacetylases: enzymes with functional diversity as novel therapeutic targets. *Prog. Cell Cycle Res.* 5:269–278.